

## Static Friction Phenomena in Granular Materials: Coulomb Law versus Particle Geometry

Thorsten Pöschel and Volkhard Buchholtz

*Hochleistungsrechenzentrum, Kernforschungsanlage Jülich, Postfach 1913, D-52425 Jülich, Germany*  
*and Humboldt-Universität zu Berlin, Fachbereich Physik, Institut für Theoretische Physik,*

*Unter den Linden 6, D-10099 East Berlin, Germany*

(Received 9 August 1993)

The static as well as the dynamic behavior of granular material are determined by dynamic and static friction. There are well known methods to include static friction in molecular dynamics simulations using scarcely understood forces. We propose an ansatz based on the geometrical shape of nonspherical particles which does not involve an explicit expression for static friction. It is shown that the simulations based on this model are close to experimental results.

PACS numbers: 46.10.+z, 05.60.+w, 47.27.-i, 81.35.+k

The behavior of fluidized dry granular material, like sand or powder, reveals a rich variety of effects which cannot be observed in other substances. Those effects have been observed and investigated by many scientists over a long period [1–5]. Examples for the most interesting effects are fluidization, convection cells and heap formation under vibration [2,6–8], size segregation (“Brazil-nut” effect) [9–11], deformation under shear force [12], shape segregation of differently shaped grains in a pipe [13], and clustering instabilities [14]. Density waves emitted from outlets [15] inside material flowing through pipes [16] and at the surface of an inclined chute [17] have been intensively investigated. Of particular interest are the dynamic as well as the static behavior of avalanches going down the slope of a sandpile. Theoretical as well as experimental investigations [18–22] led to the hypothesis that their mass and their time distributions can be described by the self-organized criticality model. There are experiments, however, that do not agree with this hypothesis [6,23]. Recently many experimental observations have been reproduced by numerical simulations. There is a wide variety of simulation methods including Monte Carlo simulations (e.g., [10]), molecular dynamics simulations (e.g., [4,9,13]), and random walk approaches [24]. These simulations gave much interesting information on the microscopic effects underlying the behavior of macroscopic amounts of granular material. Many of the effects observed in experiments are consequences of static friction between the grains. In most of the current simulations special terms for static friction are used to mimic static behavior of granular material, e.g., [4,25]. The aim of this paper is to show that it is possible to reproduce the experimental results by molecular dynamics simulations without introducing such a static friction force but by simulating nonspherical particles. We show that our simulations with nonspherical particles agree better with experimental results than equivalent simulations introducing static friction forces as is usually done.

Since it is extremely complicated to calculate collisions

of cubic particles, we choose in two dimensions particles similar to squares but consisting of spheres. A further advantage of this model is that we are able to vary the shape steadily from a sphere almost to a square. A related ansatz for nonspherical grains was recently done by Gallas and Sokołowski [26]; there each grain consists of two spheres rigidly glued to each other. Each of our nonspherical particles  $k$  consists of four spheres with equal radii  $r_i^{(k)}$ , located at the edges of a square of size  $L^{(k)}$ , and one sphere with radius  $r_m^{(k)} = L^{(k)}/\sqrt{2} - r_i^{(k)}$  in the middle of the square (Fig. 1). For the case where two spheres  $i$  and  $j$  with masses  $m_i$  and  $m_j$  of the same particle  $k$  or of different particles touch each other during a collision, there acts the force

$$\mathbf{F}_{ij}^C = [Y(r_i + r_j - |\mathbf{x}_i - \mathbf{x}_j|) - \gamma m_{\text{eff}} |\dot{\mathbf{x}}_i - \dot{\mathbf{x}}_j|] \frac{\mathbf{x}_i - \mathbf{x}_j}{|\mathbf{x}_i - \mathbf{x}_j|},$$

where  $Y$  is the Young modulus,  $\gamma$  is the phenomenological friction coefficient, and  $m_{\text{eff}}$  is the effective mass  $m_{\text{eff}} = \frac{m_i m_j}{m_i + m_j}$ . In addition to the forces between every two particles of the system, there are forces between each pair of spheres  $i, j$  where  $i$  and  $j$  both belong to the same grain, due to a damped spring,

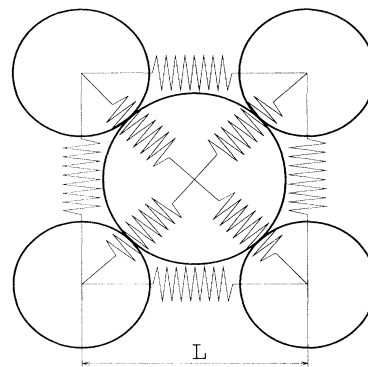


FIG. 1. Shape of a nonspherical particle.

$$\mathbf{F}_{ij}^S = \left[ \alpha(C^{(k)} - |\mathbf{x}_i - \mathbf{x}_j|) + \gamma_{sp} \frac{m_i}{2} |\dot{\mathbf{x}}_i - \dot{\mathbf{x}}_j| \right] \frac{\mathbf{x}_i - \mathbf{x}_j}{|\mathbf{x}_i - \mathbf{x}_j|},$$

where  $\alpha$  and  $\gamma_{sp}$  are the spring constant and the damping coefficient. If the spheres  $i$  and  $j$  are both located at the same edge of the square then  $C^{(k)}$  equals  $L^{(k)}$ , if  $i$  is the central sphere then  $C^{(k)} = L^{(k)}/\sqrt{2}$ . The interaction between different grains is purely geometrical without any intergrain friction.

The dynamics of large numbers of such nonspherical particles was investigated simulating the flow of granular material in a rotating cylinder under gravity. For the integration we used a sixth order predictor-corrector method [27]. In a cylinder of diameter  $D = 260$  mm we simulated the flow of 1000 nonspherical particles of different size  $L^{(k)}$  with Gaussian probability distribution  $p(L^{(k)}) = N(3, 1)$  with mean value  $\overline{L^{(k)}} = 3$  mm, each consisting of five spheres. For the parameters we chose  $Y = 10^4$  kg/s<sup>2</sup>,  $\gamma = 1.5 \times 10^4$  s<sup>-1</sup>,  $\alpha = 10^4$  kg/s<sup>2</sup>,  $\gamma_{sp} = 3 \times 10^4$  s<sup>-1</sup>, and  $r_i^{(k)} = \frac{1}{4}L^{(k)}$ . The chosen parameters are typical for a soft granular material. The cylinder consists of spheres with different radii to mimic a rough surface. The mean value of these spheres equals the mean value of the  $L^{(k)}$ . The cylinder was rotated clockwise with very low uniform angular velocity  $\Omega$ . The time evolution of the slope  $\Theta$  of the surface as well as the averaged velocity  $\bar{v}$  of the particles at the surface for a fixed angular velocity  $\Omega = 0.002$  s<sup>-1</sup> are drawn in Fig. 2 [curves  $v(a)$ ,  $\Theta(a)$ ]. The angle was plotted in rad,  $\bar{v}$  in 50 s<sup>-1</sup>. Since the number of particles is not too large, our surfaces are not smooth. Hence we have to determine the inclination indirectly as the angle between the straight line connecting the center of mass point of the grains and the middle point of the rotating cylinder and the direction of gravity. The angle and particularly the average velocity of the surface particles fluctuate drastically and irregularly as is typical for stick-slip motion. This behavior was observed experimentally before by Briscoe, Pope, and Adams [28] and by Rajchen-

bach [29]. The plots  $v(b)$ ,  $\Theta(b)$  in the same figure show the equivalent data for the simulation using spherical particles. The radii of the spheres were Gauss distributed too with  $p(r_i) = N[1, 1]$ . The spherical grains undergo the same force as the spheres of which the nonspherical particles consist. To mimic static friction we include for the case of spherical particles rotation as a further degree of freedom of the grains and add the force

$$\mathbf{F}_{ij}^{sf} = \min\{-\gamma_s m_{\text{eff}} |\mathbf{v}_{\text{rel}}|, \mu |\mathbf{F}_{ij}^C|\} \begin{pmatrix} 0 & -1 \\ 1 & 0 \end{pmatrix} \frac{\mathbf{x}_i - \mathbf{x}_j}{|\mathbf{x}_i - \mathbf{x}_j|}$$

with

$$\mathbf{v}_{\text{rel}} = (\dot{\mathbf{x}}_i - \dot{\mathbf{x}}_j) + r_i \dot{\omega}_i + r_j \dot{\omega}_j,$$

where  $\dot{\omega}_i$  is the angular velocity of the  $i$ th particle,  $\gamma_s$  is the shear friction coefficient, and  $\mu$  is the Coulomb parameter ( $\gamma_s = 3 \times 10^4$  s<sup>-1</sup>,  $\mu = 0.5$ ). This ansatz is the most popular to include static friction between particles which roll on each other [4,9]. The force  $\mathbf{F}_{ij}^{sf}$  was implemented only for the simulation of spherical grains but not for the nonspherical.

Obviously the qualitative behavior of the slope  $\Theta$  in both simulations resembles each other but quantitatively we get for nonspherical grains more than twice the mean angle ( $\overline{\Theta}_{\text{ns}}$ ) than for spherical ( $\overline{\Theta}_{\text{sp}}$ ). For very low rotation velocity  $\Omega = 2 \times 10^{-3}$  s<sup>-1</sup> we found  $\overline{\Theta}_{\text{sp}} = 7^\circ$  and  $\overline{\Theta}_{\text{ns}} = 19^\circ$ . In the experiment [29]  $\Theta \approx 27^\circ$  was measured. The average velocity of the surface grains differs significantly too for both cases. The typical avalanches in the case of nonspherical particles cannot be observed for spheres. The curve  $\bar{v}(b)$  is much smoother. In the experiment one observes stick-slip motion [29]. Figure 3 shows the slope  $\Theta$  of the surface as a function of the angular velocity of the cylinder  $\Omega$  for both nonspherical and spherical grains. In both cases the curves are close to a straight line. For much higher angular velocities than used in our simulations the grains do not move stick slip like but continuously. In this regime,  $\Omega \sim (\Theta - \Theta_c)^l$ , with  $l = 0.5 \pm 0.1$ , was found experimentally [29]. With the same ansatz we find  $l \approx 1.25$  for the stick-slip regime. As

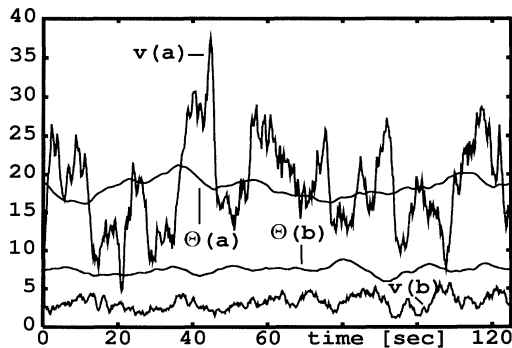


FIG. 2. Time evolution of the slope  $\Theta$  of the surface and the averaged velocity  $\bar{v}$  of the particles at the surface of the flow for nonspherical (a) and spherical (b) grains.

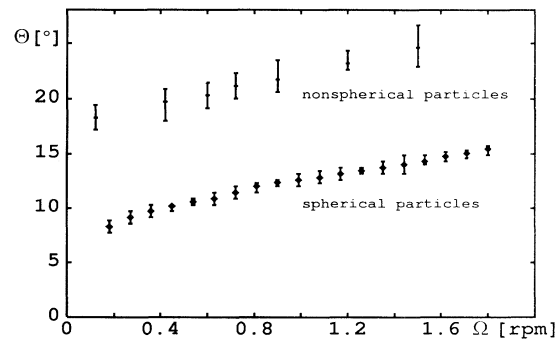


FIG. 3. The inclination  $\Theta$  of the surface as a function of the angular velocity  $\Omega$  of the cylinder.

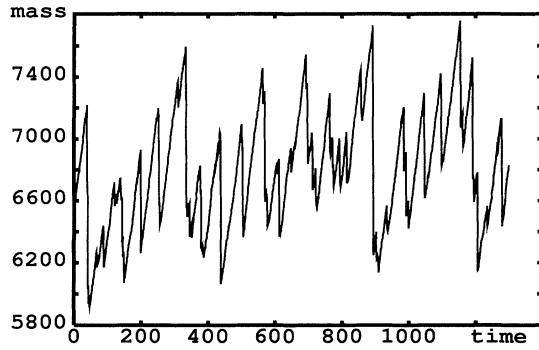


FIG. 4. Total mass of a pile of nonspherical grains on a platform of finite length  $P = 820$ .

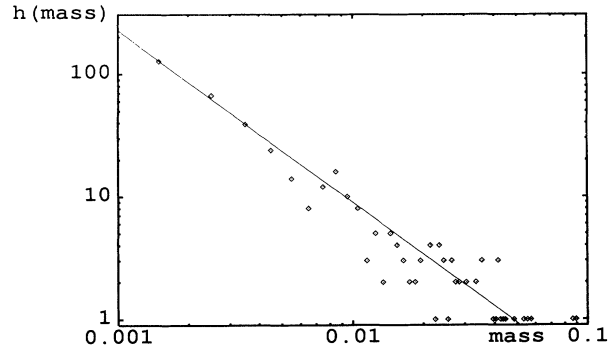


FIG. 5. Size distribution of the avalanches. The line displays the function  $h(N_A) = (N_A)^{-1.4}$ .

shown above the simulation with nonspherical grains coincides much better with the experimental observations than with equivalent simulations using spheres.

In our second simulation we investigate the evolution of a stable pile of granular material by continuously dropping particles on the top of the pile due to the experiment of Held *et al.* [20]. Beginning with an empty rough plane we drop the next particle when the maximum velocity vanishes,  $v_{\max} \ll 1$ . The rough plane was simulated by a chain of fixed spheres of random radii with mean  $\bar{r}_i = \bar{L}^{(i)}$ . The parameters of the simulation were the same as in the previous experiment.

During the simulation we noticed that the slope of a pile of nonspherical grains does not depend on the number of particles. For spherical grains, however, the heap dissolves under gravity with increasing particle number. There are molecular dynamics simulations of stable piles with spherical grains, e.g., [25], but there the particles are not allowed to roll on each other, hence they can only slide; this behavior does not correspond to experimental reality.

If the platform above which the heap is built up has a finite length  $P$  one can investigate the fluctuations of the mass  $m_h$  of a heap of definite size and the distribution of the size of the avalanches, i.e., the mass fluctuations of the heap. In Fig. 4 the time series of the mass  $m_h$  is drawn for fixed  $P$ . The mass fluctuates irregularly due to avalanches of different size going down the surface of the heap. The size distribution of the avalanches follows a power law; Fig. 5 shows the spectrum. For the exponent  $h(N_A) \sim (N_A)^l$  we found  $l \approx -1.4$ . The experiments yield  $l \approx -2.5$  [20] and  $l \approx -2.134$  [21]. For the case of spherical grains we cannot find avalanches.

The ratio between the size of a grain and the radii of the spheres at the corners determines whether the grains shape is closer to a sphere or to a square. Hence we define a shape value  $S = 1 - R_{\min}^{cc}/R_{\max}^{cc}$ , where  $R_{\min}^{cc}$  and  $R_{\max}^{cc}$  are the extremal values of the distance between the convex cover of the nonspherical grain and its central point (Fig. 6). For the limit  $S \rightarrow 0$  the grains have

the shape of spheres. The function reaches its maximum  $S_m = 0.255$  for a grain whose convex cover is most similar to that of a square. In order to ensure that the mass of a grain is independent of  $S$  we scale its density  $\rho$  due to its shape. Figure 6 shows the angle of the heap as a function of the shape  $S$ . For grains with shape  $S = S_m$ , which corresponds to  $(L^{(k)}/r_i^{(k)})_{S_m} = 9.66$ , the inclination of the heap reaches a maximum too. The angle  $\Phi \approx 23.1^\circ$  agrees with experimental data; Bretz *et al.* [21] found  $\Phi \approx 25^\circ$ . Each other value of  $S$  corresponds to two different particle shapes, both closer to a sphere than the  $S_m$  particle. The values marked by  $\odot$  are due to grains with  $L^{(k)}/r_i^{(k)} \leq (L^{(k)}/r_i^{(k)})_{S_m}$ , + designates the slope of the heap for particles with  $L^{(k)}/r_i^{(k)} \geq (L^{(k)}/r_i^{(k)})_{S_m}$ . As expected the slope  $\Phi$  of the heap rises with growing  $L^{(k)}/r_i^{(k)}$  until  $S$  reaches its maximum  $S_m$ . For larger ratio  $L^{(k)}/r_i^{(k)}$  ( $S < S_m$ ) the slope  $\Phi$  decreases. The dashed line in Fig. 6 displays the inclination  $\Phi_{sp}$  we measured for

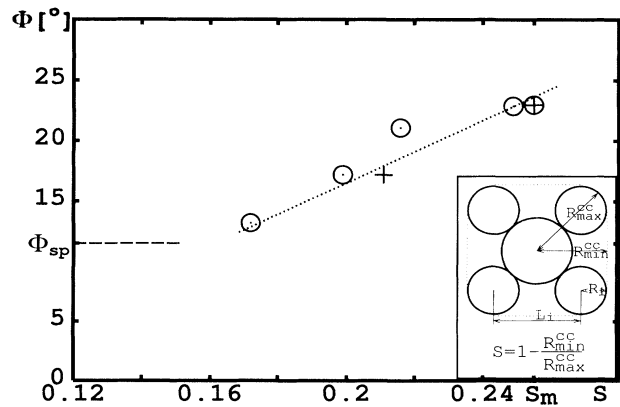


FIG. 6. Slope  $\Phi$  of a heap over the shape value  $S$  for grains with  $L^{(k)}/r_i^{(k)} \leq (L^{(k)}/r_i^{(k)})_{S_m}$  ( $\odot$ ) and  $L^{(k)}/r_i^{(k)} \geq (L^{(k)}/r_i^{(k)})_{S_m}$  (+). The dotted line leads the eye to the function  $\Phi = 130S + \text{const}$ . The dashed line displays the inclination observed in simulation with spherical particles.

a heap of spheres, which corresponds to  $S \rightarrow 0$ .  $\Phi_{sp}$  gives a lower boundary for the slope. The observed  $\Phi$  values for  $S \in (0, S_m)$  lie between  $\Phi_{sp}$  and  $\Phi(S_m)$ .

The simulations described above demonstrate that nonspherical grains are able to describe the static behavior of granular materials. It is shown that equivalent simulations with spherical grains and an additional term which describes the static friction due to the Coulomb law could reproduce the experimental results neither for stick-slip motion nor for the angle of repose of a sandpile. The angle of repose reaches its extremal value for grains whose shape is close to a square.

Hence we conclude that our microscopic model of nonspherical grains supplies a possible description of the static behavior of a granular material. The results regarding nonsphericity agree well with those in [26].

The authors thank J. A. C. Gallas and H. J. Herrmann for stimulating and enlightening discussions.

- 
- [1] C. A. Coulomb, *Acad. R. Sci. Mem. Math. Phys. par Divers Savants* **7**, 343 (1773).
- [2] M. Faraday, *Philos. Trans. R. Soc. London* **52**, 299 (1831).
- [3] Hagen, *Verhandl. Königl. Preuss. Akad.* p. 35 (1852).
- [4] P. Cundall and O. D. L. Strack, *Géotechn.* **29**, 47 (1979).
- [5] H. M. Jaeger and S. Nagel, *Science* **255**, 1523 (1992).
- [6] P. Evesque and J. Rajchenbach, *Phys. Rev. Lett.* **62**, 44 (1989); C. Laroche, S. Douady, and S. Fauve, *J. Phys. (Paris)* **50**, 699 (1989); P. Evesque, *J. Phys. (Paris)* **51**, 697 (1990); J. Rajchenbach, *Europhys. Lett.* **16**, 149 (1991).
- [7] F. Dinkelacker, A. Hübler, and E. Lüscher, *Biol. Cybern.* **56**, 51 (1987); J. Walker, *Sci. Am.* **247**, 167 (1982); P. Evesque, E. Szmatala, and J.-P. Denis, *Europhys. Lett.* **12**, 623 (1990); E. Clement and J. Rajchenbach, *Europhys. Lett.* **16**, 133 (1991); H. J. Herrmann, *Physica (Amsterdam)* **191A**, 263 (1992); P. Evesque and W. Meftah (to be published).
- [8] J. A. C. Gallas, H. J. Herrmann, and S. Sokolowski, *Phys. Rev. Lett.* **69**, 1371 (1992); *J. Phys. (Paris)* **2**, 1389 (1992); Y. H. Taguchi, *Phys. Rev. Lett.* **69**, 1367 (1992); *J. Phys. (Paris)* **2**, 2103 (1992); Report No. titcmt-1992-7, 1992 (unpublished); *J. Mod. Phys. B* **7**, 1839 (1993).
- [9] P. K. Haff and B. T. Werner, *Powder Technol.* **48**, 239 (1986).
- [10] P. Devillard, *J. Phys. (Paris)* **51**, 369 (1990).
- [11] J. C. Williams, *Powder Technol.* **15**, 245 (1976); A. Rosato, K. J. Strandburg, F. Prinz, and R. H. Swendsen, *Phys. Rev. Lett.* **58**, 1038 (1987); *Powder Technol.* **49**, 59 (1986); R. Jullien, P. Meakin, and A. Pavlovitch, *Phys. Rev. Lett.* **69**, 640 (1992); T. Ohtsuki, Y. Takemoto, and A. Hayashi (to be published).
- [12] S. B. Savage, *J. Fluid Mech.* **92**, 53 (1979); H. M. Jaeger, C. Liu, S. R. Nagel, and T. A. Witten, *Europhys. Lett.* **11**, 619 (1990); P. A. Thompson and G. S. Grest, *Phys. Rev. Lett.* **67**, 1751 (1991).
- [13] S. Sokolowski and H. J. Herrmann, *Europhys. Lett.* **18**, 415 (1992).
- [14] I. Goldhirsch and G. Zanetti, *Phys. Rev. Lett.* **70**, 1619 (1993).
- [15] G. W. Baxter, R. P. Behringer, T. Fagert, and G. A. Johnson, *Phys. Rev. Lett.* **62**, 2825 (1989); O. Cutress and R. F. Pulfer, *Powder Technol.* **1**, 213 (1967); A. Drescher, T. W. Cousens, and P. L. Bransby, *Geotechnol.* **28**, 27 (1978); G. Ristow and H. J. Herrmann, Report No. HLRZ 2/93, 1993 (unpublished); G. Ristow, *J. Phys. (Paris)* **2**, 649 (1991); G. W. Baxter and R. P. Behringer, *Physica (Amsterdam)* **51D**, 465 (1991); *Phys. Rev. A* **42**, 1017 (1990); D. C. Hong and J. A. McLennan, *Physica (Amsterdam)* **187A**, 159 (1992).
- [16] K. L. Schick and A. A. Verveen, *Nature (London)* **251**, 599 (1974); Y. Tsuji, T. Tanaka, and T. Ishida, *Powder Technol.* **71**, 239 (1992); T. Pöschel, Report No. HLRZ 67-92, 1992 (unpublished).
- [17] T. G. Drake, *J. Fluid Mech.* **199**, 177 (1989); **225**, 121 (1991); S. B. Savage and K. Hutter, *J. Fluid Mech.* **199**, 177 (1989); O. Walton, Report UCRL-JL-10834, 1992 (unpublished); T. Pöschel, *J. Phys. (Paris)* **3**, 27 (1993).
- [18] P. Bak, C. Tang, and K. Wiesenfeld, *Phys. Rev. Lett.* **59**, 381 (1987).
- [19] L. P. Kadanoff, S. R. Nagel, S. R. Wu, and S. Zhou, *Phys. Rev. A* **39**, 6524 (1989).
- [20] G. A. Held, D. H. Solina, D. T. Keane, W. J. Haag, P. M. Horn, and G. Grinstein, *Phys. Rev. Lett.* **65**, 1120 (1990).
- [21] M. Bretz, J. B. Cunningham, P. L. Kurczynski, and F. Nori, *Phys. Rev. Lett.* **69**, 2431 (1992).
- [22] D. Dhar and R. Ramaswamy, *Phys. Rev. Lett.* **63**, 1659 (1990); T. Hwa and M. Kardar, *Phys. Rev. Lett.* **62**, 1813 (1989); B. McNamara and K. Wiesenfeld, *Phys. Rev. A* **41**, 1867 (1990); C. Tang and P. Bak, *J. Stat. Phys.* **51**, 797 (1988); E. N. Miranda and H. J. Herrmann, *J. Phys. A* **175**, 339 (1991); K. Wiesenfeld, J. Theiler, and B. McNamara, *Phys. Rev. Lett.* **65**, 949 (1990).
- [23] H. M. Jaeger, C. Liu, and S. Nagel, *Phys. Rev. Lett.* **62**, 40 (1989); S. R. Nagel, *Rev. Mod. Phys.* **64**, 321 (1992).
- [24] H. Caram and D. C. Hong, *Phys. Rev. Lett.* **67**, 828 (1991).
- [25] J. Lee, Report No. HLRZ 71-92, 1992 (unpublished).
- [26] J. A. C. Gallas and S. Sokolowski, *Int. J. Mod. Phys. B* **7**, 2037 (1993).
- [27] M. P. Allen and D. J. Tildesley, *Computer Simulations of Liquids* (Clarendon Press, Oxford, 1987).
- [28] B. J. Briscoe, L. Pope, and M. J. Adams, *Powder Technol.* **37**, 169 (1984).
- [29] J. Rajchenbach, *Phys. Rev. Lett.* **65**, 2221 (1990).